SPIN AND CHARGE ORDER IN THE VORTEX LATTICE OF THE CUPRATES: EXPERIMENT AND THEORY

Subir Sachdev

Department of Physics, Yale University,

P.O. Box 208120, New Haven CT 06520-8120, USA

Email: subir.sachdev@yale.edu; Web: http://pantheon.yale.edu/~subir

Date: February 15, 2002; updated October 15, 2003

Abstract I summarize recent results, obtained with E. Demler, K. Park, A. Polkovnikov, M. Vojta, and Y. Zhang, on spin and charge correlations near a magnetic quantum phase transition in the cuprates. STM experiments on slightly overdoped $Bi_2Sr_2CaCu_2O_{8+\delta}$ (J. E. Hoffman *et al.*, Science **295**, 466 (2002)) are consistent with the nucleation of static charge order coexisting with dynamic spin correlations around vortices, and neutron scattering experiments have measured the magnetic field dependence of static spin order in the underdoped regime in $La_{2-\delta}Sr_\delta CuO_4$ (B. Lake *et al.*, Nature **415**, 299 (2002)) and $LaCuO_{4+y}$ (B. Khaykovich *et al.*, Phys. Rev. B **66**, 014528 (2002)). Our predictions provide a semi-quantitative description of these observations, with only a single parameter measuring distance from the quantum critical point changing with doping level. These results suggest that a common theory of competing spin, charge and superconducting orders provides a unified description of all the cuprates.

Keywords: Spin density wave, charge density wave, superconductivity, vortex lattice

Mexican Meeting on Mathematical and Experimental Physics, Collegio Nacional, Mexico City, September 2001. Published in *Developments in Mathematical and Experimental Physics, Volume B: Statistical Physics and Beyond*, A. Macias, F. Uribe, and E. Diaz eds, Kluwer Academic, New York (2002);

Introduction

Three recent experiments [1, 2, 3] have shed new light on the spin and charge density wave collective modes of the cuprate superconductors. This article will summarize the main results of our theory [4, 5, 6, 7, 8, 9, 10] of these collective modes in the vicinity of a quantum phase transition between two superconducting states, only one of which has static, long-range, spin density wave order: we will recall our main predictions, and discuss further experimental tests. we will also connect our theory to these experiments. In particular, we suggested [6] that static charge order should coexist with dynamic spin-gap fluctuations around the vortex cores in the cuprate superconductors, as may have been been observed in [1]. We also discussed [5] a singular field dependence for the static magnetic moment in the underdoped cuprates, and this is consistent with [2, 3].

The starting hypothesis of our theory is that the collective spin excitations of the doped cuprates can be described by using the proximity of a magnetic quantum critical point. This was proposed in Ref. [11]; almost simultaneously, NMR experiments in $La_{2-\delta}Sr_{\delta}CuO_4$ [12] showed crossovers which could be neatly interpreted in terms of a magnetic quantum critical point near a doping concentration $\delta \approx 0.12$ with dynamic exponent $z = 1$. The ground state is a good superconductor at this value of δ, and so the magnetic transition takes place between two superconducting states. Evidence supporting this interpretation also appeared in neutron scattering measurements [13]. An explicit theory for a quantum transition between a d-wave superconductor with co-existing long-range spin density wave order (a SC+SDW state) and an ordinary d-wave superconductor (a SC state) was first discussed by Balents *et al.* [14]; they focused on the case where the SDW ordering wavevector was exactly equal to the spacing between the two nodal points where the d-wave superconductor has gapless quasi-particle excitations, and studied their role in the critical theory. However, their analysis also makes it clear that the nodal quasiparticles can be safely neglected for the generic case in which the wavevector matching condition is not satisfied [4], and we will mainly discuss this simpler case here. The SC+SDW to SC transition in this case is formally identical to that in an insulator, and the SC state has a sharp $S = 1$ 'resonance peak' associated with stable $S = 1$ collective excitonic excitation [15]. Such a theory for the SC to SC+SDW transition was used by us [16] to predict the effects of Zn impurities on the resonance peak in the SC phase.

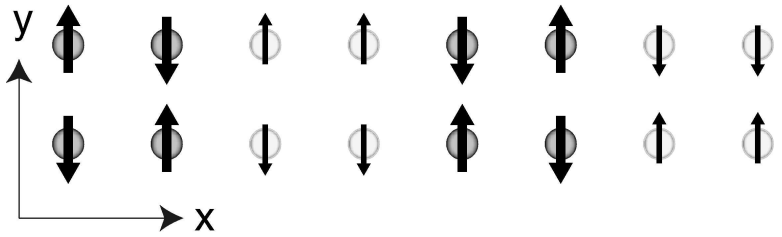

Figure 1. A bond-centered, collinear SDW at the wavevector $(3\pi/4, \pi)$. The size of the arrow represents the mean spin moment, while the shading of the circle is the electron density. The sliding degree of freedom corresponds to a shift in the position of the light and dark circles.

1. ORDER PARAMETER AND FIELD THEORY

Neutron scattering experiments show that the lowest energy collective spin excitations at and above $\delta \approx 0.12$ reside near the wavevectors $\mathbf{K}_x = (3\pi/4, \pi)$ and $\mathbf{K}_y = (\pi, 3\pi/4)$ (our unit of length is the square lattice spacing). So we write for the spin operator at the site $\mathbf{r}$:

$$S_\alpha(\mathbf{r}, \tau) = \mathrm{Re}\left[e^{i\mathbf{K}_x\cdot\mathbf{r}}\Phi_{x\alpha}(\mathbf{r}, \tau) + e^{i\mathbf{K}_y\cdot\mathbf{r}}\Phi_{y\alpha}(\mathbf{r}, \tau)\right], \tag{1}$$

where $\alpha = x, y, z$ extends over the directions in spin space, and $\Phi_{x,y\alpha}$ are *complex* fields which will serve as order parameters for the SC+SDW to SC transition. In the SC+SDW phase, $\Phi_{x,y\alpha}$ are condensed and the condensate describes the spatial modulation of the spin, by (1); in the SC phase, the $\Phi_{x,y\alpha}$ are dynamically fluctuating, and its quanta are *spin excitons*. The representation (1) can describe a large variety of spin modulations *e.g.* the state with $\langle\Phi_{x\alpha}\rangle \propto (1, i, 0)$, $\langle\Phi_{y\alpha}\rangle = 0$ is a spiral SDW in the x direction. Experimentally, however, it is clear that the SDW is not spiral, but *collinear*; an example of a collinear SDW has $\langle\Phi_{x\alpha}\rangle \propto e^{i\theta}(1, 0, 0)$, $\langle\Phi_{y\alpha}\rangle = 0$—notice that the average spin vectors on all sites are parallel or antiparallel. The phase θ represents a *sliding* degree of freedom of the SDW: for the special commensurate value of $\mathbf{K}_x$ under consideration here, the coupling to the lattice will prefer that θ take one of the values $n\pi/4$ (a site-centered SDW) or $(n + 1/2)\pi/4$ (a bond-centered SDW) where $n = 0 \ldots 7$ integer. A sketch of a bond-centered SDW is shown in Fig 1. Notice that the magnitude of the spin changes from site to site, and this implies [17] that there must be a corresponding modulation in the electron density, $\delta\rho(\mathbf{r})$: the latter has the same quantum numbers as $\sum_\alpha S_\alpha^2$, and hence we deduce that the

charge order can be written as

$$\delta\rho(\mathbf{r},\tau) \propto \mathrm{Re}\sum_{\alpha}\left[e^{i2\mathbf{K}_x\cdot\mathbf{r}}\Phi^2_{x\alpha}(\mathbf{r},\tau) + e^{i2\mathbf{K}_y\cdot\mathbf{r}}\Phi^2_{y\alpha}(\mathbf{r},\tau)\right] + \ldots . \quad (2)$$

The period of the charge order is half that of the SDW, and the amplitude of the charge order vanishes for the spiral SDW. We emphasize that after accounting for the long-range Coulomb interactions, the actual modulation in the electron charge density per site may well be unobservably small. The "charge order" discussed here and in (2) should be interpreted in a much more general sense, as representing a modulation at wavevectors $2\mathbf{K}_{x,y}$ in all spin-singlet observables which are invariant under time-reversal; the modulation could be larger in other observables like the mean kinetic energy, exchange energy, or pairing amplitude in the bonds between nearest-neighbor sites.

We are interested here in the quantum transition from the SC+SDW state with $\langle\Phi_{x,y\alpha}\rangle \neq 0$ to the SC state with $\langle\Phi_{x,y\alpha}\rangle = 0$ in a background of quiescent superconductivity. The allowed terms in the effective action are constrained by the underlying symmetries: these were discussed in some generality in [9]. Here we will be satisfied by considering a simplified effective action which is written most easily in terms of the real and imaginary components of $\Phi_{x,y\alpha}$:

$$\begin{array}{lll} \Phi_{xx} = \varphi_1 + i\varphi_7 & \Phi_{xy} = \varphi_2 + i\varphi_8 & \Phi_{xz} = \varphi_3 + i\varphi_9 \\ \Phi_{yx} = \varphi_4 + i\varphi_{10} & \Phi_{yy} = \varphi_5 + i\varphi_{11} & \Phi_{yz} = \varphi_6 + i\varphi_{12} \end{array} \quad (3)$$

The effective action for the real fields φ_μ, $\mu = 1 \ldots 12$ is taken to be

$$\mathcal{S}_\varphi = \int d^2r d\tau \Big\{ \frac{1}{2}\Big[(\partial_\tau\varphi_\mu)^2 + (\nabla_{\mathbf{r}}\varphi_\mu)^2 + s\varphi_\alpha^2\Big] + \frac{u}{2}(\varphi_\mu^2)^2 \Big\} \quad (4)$$

where a summation over the repeated μ index is implied, and we have chosen units so that the velocity of spin waves is unity. Notice that the action $\mathcal{S}_\varphi$ has a large O(12) symmetry of rotations in μ space. This symmetry is present in *all* allowed terms which are quadratic in φ_μ, but is broken by a number of quartic terms [9] which are not displayed in (4). However, all permitted terms in the effective action do respect the sliding symmetry under which $\Phi_{x,y\alpha} \to e^{in_{x,y}\pi/4}\Phi_{x,y\alpha}$ for integer $n_{x,y}$. The coupling s serves as the tuning parameter which measures distance from the quantum critical point: the SC+SDW phase will appear for $s < s_c$ and the spin-singlet SC phase for $s > s_c$. The dynamic properties of the transition at $s = s_c$ have been investigated in much detail in earlier work [15].

Now we consider the influence of the magnetic field, H, applied perpendicular to the CuO_2 layers. This couples most strongly to the 'background' SC order, and so we are forced to consider the response of the

superconducting order parameter $\psi(\mathbf{r})$. In suitable units (discussed in [9]), the free energy for $\psi(\mathbf{r})$ can be written in the familiar Ginzburg-Landau form

$$\mathcal{F} = \Upsilon \int d^2r \left[-|\psi|^2 + \frac{1}{2}|\psi|^4 + |(\nabla_{\mathbf{r}} - i\mathbf{A})\,\psi|^2 \right]. \tag{5}$$

where Υ is a parameter measuring the relative contributions of the magnetic and superconducting energies, and $\nabla_{\mathbf{r}} \times \mathbf{A} = H\hat{\mathbf{z}}$. Notice that we have assumed a τ independent ψ—this is permissible because the SC order is non-critical and its quantum fluctuations can be safely neglected.

Finally, we have to couple the H-response of $\psi(\mathbf{r})$ to the quantum SDW fluctuations. There are two distinct couplings, which have rather different physical consequences. The first, v, is a simple coupling between the magnitudes of the SC and SDW order parameters, chosen with a repulsive sign ($v > 0$) to account for the competition between these orders:

$$\mathcal{S}_v = \frac{v}{2} \int d^2r d\tau \varphi_\mu^2(\mathbf{r},\tau)|\psi(\mathbf{r})|^2. \tag{6}$$

Such a coupling was discussed by Zhang [18], in work focusing on the possibility of a *first order* transition between an SC phase and an insulating phase with SDW order. The coupling v will play an important role in determining our phase diagram to be described below, which contains a *second order* transition between SC and SC+SDW phases. The second coupling, unlike v, recognizes the fact that the vortex lattice induced by H breaks translational symmetry, and so the SDW fluctuations should also not be invariant under the 'sliding' symmetry (the term in (6) is invariant under the sliding symmetry). In particular the vortex core radius in the cuprates is only of the order of a few lattice spacings, and the energy of an SDW fluctuation will certainly change depending upon which portion of the charge order (see Fig 1) is centered on a vortex core. In other words, each vortex core, at a position $\mathbf{r}_v$, will prefer a certain phase of the local charge order parameter $\sum_\alpha \Phi^2_{x,y\alpha}(\mathbf{r}_v,\tau)$. Expanding the charge order parameter using (3), we deduce the second term which couples the SC and SDW order parameters:

$$\mathcal{S}_{\rm pin} = -\sum_{\{\mathbf{r}_v,\psi(\mathbf{r}_v)=0\}} \int d\tau \Bigg\{ \sum_{\mu=1}^{3} \mathrm{Re}\Big[\zeta_x \left(\varphi_\mu(\mathbf{r}_v,\tau) + i\varphi_{6+\mu}(\mathbf{r}_v,\tau)\right)^2\Big] + \sum_{\mu=4}^{6} \mathrm{Re}\Big[\zeta_y \left(\varphi_\mu(\mathbf{r}_v,\tau) + i\varphi_{6+\mu}(\mathbf{r}_v,\tau)\right)^2\Big] \Bigg\}. \tag{7}$$

The complex coupling constants $\zeta_{x,y}$ measure the pinning strength of the phase of the sliding charge order to some preferred value near each vortex core.

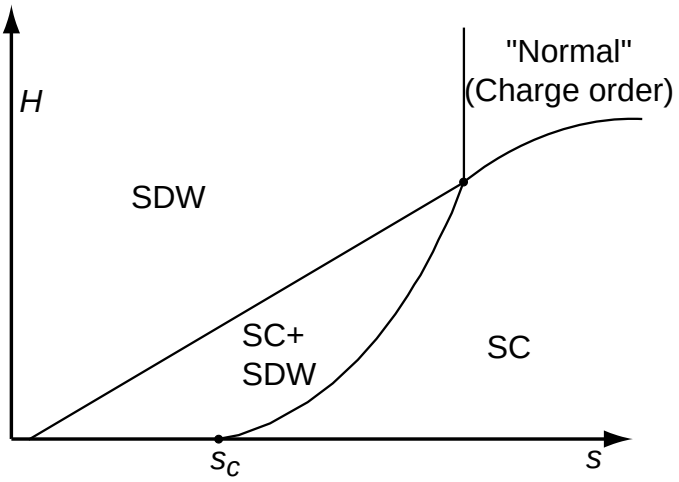

Figure 2. Zero temperature phase diagram of the model $\mathcal{Z}$ defined in (8) and (9); from Refs. [5] and [9]. The phases have the following expectation values: (*i*) SC: $\langle\varphi_\mu\rangle = 0$, $\langle\psi\rangle \neq 0$, (*ii*) SC+SDW: $\langle\varphi_\mu\rangle \neq 0$, $\langle\psi\rangle \neq 0$, (*iii*) SDW: $\langle\varphi_\mu\rangle \neq 0$, $\langle\psi\rangle = 0$, and (*iv*) "Normal": $\langle\varphi_\mu\rangle = 0$, $\langle\psi\rangle = 0$.

We have now defined a well-posed field theoretical problem, which was analyzed in some detail in [9]: describe the dynamic quantum SDW fluctuations associated with the partition function

$$\mathcal{Z}\left[\psi(\mathbf{r})\right] = \int \mathcal{D}\varphi_\mu(\mathbf{r},\tau) \exp\left(-\frac{\mathcal{F}}{T} - \mathcal{S}_\varphi - \mathcal{S}_v - \mathcal{S}_{\text{pin}}\right), \tag{8}$$

where the optimum value of the static SC order $\psi(\mathbf{r})$ is determined by the minimization of $-\ln \mathcal{Z}\left[\psi(\mathbf{r})\right]$ via the solution of the saddle-point equation

$$\frac{\delta \ln \mathcal{Z}\left[\psi(\mathbf{r})\right]}{\delta\psi(\mathbf{r})} = 0. \tag{9}$$

Note the highly asymmetric treatment of the SC and SDW orders.

2. PHASE DIAGRAM

Our primary results for the properties of (8) and (9) are contained in the phase diagram as a function of s and H in Fig 2. The formal solution of these equations also allows solutions in which the SC order vanishes and $\psi(\mathbf{r}) = 0$ everywhere: this leads to the SDW phase and the "Normal" phase. However we do not expect our theory to be accurate such a regime: quantum fluctuations of the SC order parameter are surely important once $\psi(\mathbf{r})$ becomes small, and these have been neglected in our theory. Our results are more precise in the small H region of

Fig 2, in the vicinity of the boundary between the SC+SDW and SC phases; indeed, the functional forms of the main results quoted below are expected to be exact. Upon accounting for the quantum fluctuations of the superconducting order, and the Berry phases associated with the electrons in the nearby Mott insulator [4], we expect that the "Normal" phase will display some sort of static charge order.

An important prediction of our theory is the shape of the second-order phase boundary between the SC and SC+SDW phases at small H. This transition is associated with the condensation of the φ_μ exciton, when the spin gap to the creation of an exciton vanishes in the SC phase. Detailed arguments were presented in [5, 9] showing that this condensation occurs in an exciton state which is extended throughout the entire lattice; indeed, a variational approximation in which the exciton wavefunction is assumed to be simply a constant gives essentially exact results (as opposed to an approximation in which the exciton is strongly localized in the vortex cores [19]). The presence of the vortex lattice in $\psi(\mathbf{r})$ influences the energy of this extended exciton primarily via the v coupling in $\mathcal{S}_v$. When spatially averaged over $\mathbf{r}$, the dominant change in the average value of $|\psi(\mathbf{r})|^2$, and hence in the energy of the exciton, arises from slight suppression of superconductivity in the *superflow* region surrounding each vortex core. The much smaller vortex core region always has a significantly weaker effect on the exciton energy. It is a simple matter to compute the correction to the exciton energy from the superflow. The average kinetic energy of the superflow is known from standard Ginzburg-Landau theory to be $\sim (H/H_{c2}) \ln(H_{c2}/H)$ (here H_{c2} is the upper critical field at which superconductivity disappears), and the coupling v in (6) therefore leads to a corresponding change in the effective value of s controlling the exciton energy:

$$s_{\rm eff} = s - \mathcal{C} \frac{H}{H_{c2}} \ln\left(\frac{H_{c2}}{H}\right), \tag{10}$$

where $\mathcal{C}$ is a positive constant. The critical field at which the spin gap vanishes is therefore determined by $s_{\rm eff} = s_c$, and this leads to our result [5, 9] for the phase boundary between the SC and SC+SDW phases:

$$H \sim \frac{(s - s_c)}{\ln(1/(s - s_c))}. \tag{11}$$

Note that the phase boundary approaches the $H = 0$ limit with vanishing slope: consequently a relatively small field applied to the superconductor for $s > s_c$ will drive the system into the SC+SDW phase. This is our explanation for the shift in the energy of the dynamic spin fluctuations seen in [20].

The phase diagram of Fig 2 leads to a number of predictions [5, 6, 9] for observables in the SC and SC+SDW phases, some of which have been tested in recent experiments [1, 2, 3]. We discuss theory and experiment in the two phases in turn in the following subsections.

2.1. STATIC CHARGE ORDER IN THE SC PHASE

The SC phase has $\langle \varphi_\mu \rangle = 0$, and so the SDW fluctuations are dynamic and the spin exciton only exists above a finite energy gap Δ. The superconducting order $\psi(\mathbf{r})$ is suppressed in the vortex cores, and so this region should exhibit characteristics of the doped spin-gap (*i.e.* paramagnetic) Mott insulator, as was argued in [21]. Paramagnetic Mott insulators, and their response to doping with mobile charge carriers, were studied at some length in [4]: it was argued that the most likely candidates had bond-centered charge order which survived in a superconducting state for a finite range of doping—this work will be reviewed further in Section 3. Reasoning in this manner, Ref. [6] predicted that static charge order should appear in and around the vortex cores, coexisting with dynamic spin fluctuations in the SC state. Order of this type appears to have been seen in the recent STM experiment on $Bi_2Sr_2CaCu_2O_{8+\delta}$ [1]. Our approach should be contrasted from other recent investigations [22] which have *both* static spin and charge order in the vortex core.

The spatial extent of the charge order was computed in the field theory in (8), (9) in [9]. The gapped spin exciton, φ_μ, views the vortex lattice as a periodic potential, and consequently its dispersion develops the Bloch structure of a particle moving in a periodic potential. To zeroth order in the pinning terms, $\zeta_{x,y}$, the two-point ϕ_μ Green's function is diagonal in the μ index, and its diagonal component can be written as [5, 9]

$$G_\varphi(\mathbf{r}, \mathbf{r}', \omega_n) = \sum_\mu \int_{1BZ} \frac{d^2k}{4\pi^2} \frac{\Xi^*_{\mu\mathbf{k}}(\mathbf{r}) \Xi_{\mu\mathbf{k}}(\mathbf{r}')}{\omega_n^2 + E_\mu^2(\mathbf{k})}, \tag{12}$$

where $\mathbf{k}$ is a Bloch momentum which extends over the first Brillouin zone of the vortex lattice, μ is a 'band' index, $\Xi_{\mu\mathbf{k}}(\mathbf{r})$ are the Bloch states ($\Xi_{\mu\mathbf{k}}(\mathbf{r}+\mathbf{R}_v) = e^{i\mathbf{k}\cdot\mathbf{R}_v} \Xi_{\mu\mathbf{k}}(\mathbf{r})$ where $\mathbf{R}_v$ is an vector connecting two vortex centers), $E_\mu(\mathbf{k})$ are the energy dispersions of the various bands, and ω_n is an imaginary Matsubara frequency. The lowest energy exciton has energy $E_0(\mathbf{0}) \equiv \Delta$ and wavefunction $\Xi_{0\mathbf{0}}(\mathbf{r})$; this wavefunction is sketched for typical parameter values in Fig 3.

Now let us consider the influence of the pinning term in (7). Combining (7) with (2) it is simple to see that to first order in the $\zeta_{x,y}$, static

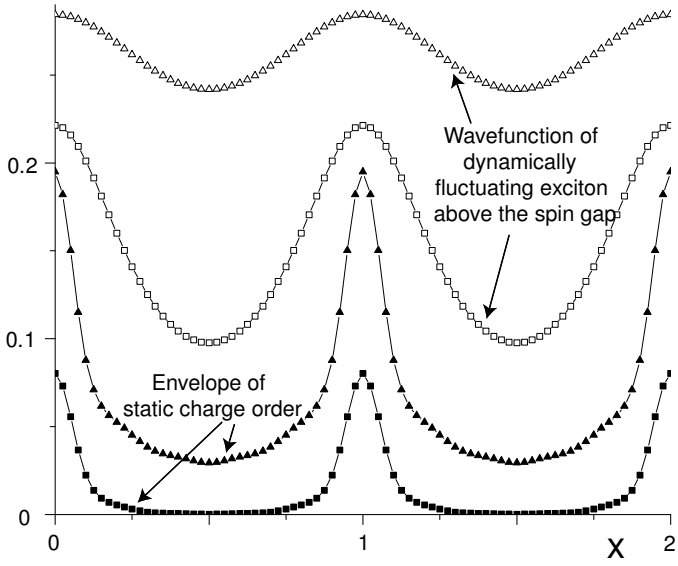

Figure 3. Spatial structure of the spin and charge correlations in the SC phase at two different magnetic fields (squares and triangles; the squares have the lower field). The vortices are centered at $x = 0, 1, 2$. The orientation of the spins fluctuates with a frequency of order the inverse spin gap $\hbar/\Delta$. The open symbols represent the lowest energy exciton wavefunction $\Xi_{00}(\mathbf{r})$. The nature of the microscopic spin correlations can be understood by recalling that this wavefunction is the envelope of the order Fig 1. After including the pinning term $\mathcal{S}_{\rm pin}$, static charge order is induced, and its envelope $\Omega(\mathbf{r})$ (defined in (13,14)) is shown above. The numerical results were obtained by Ying Zhang and reported in [9].

charge order appears in the SC phase, with

$$\langle \delta\rho(\mathbf{r}) \rangle \propto \mathrm{Re}\left[\zeta_x e^{i2\mathbf{K}_x\cdot\mathbf{r}} + \zeta_y e^{i2\mathbf{K}_y\cdot\mathbf{r}} \right] \Omega(\mathbf{r}) \tag{13}$$

where

$$\Omega(\mathbf{r}) \equiv T \sum_{\omega_n} \sum_{\mathbf{r}_v} G_\varphi^2(\mathbf{r}, \mathbf{r}_v, \omega_n). \tag{14}$$

A plot of the function $\Omega(\mathbf{r})$ is sketched in Fig 3, along with the corresponding $\Xi_{\mathbf{00}}(\mathbf{r})$. At the higher field (triangles), the spin exciton wavefunction $\Xi_{\mathbf{00}}(\mathbf{r})$ is essentially constant across the entire system, with only a weak modulation induced by the vortex lattice; nevertheless, at the same field the charge order $\Omega(\mathbf{r})$ has a strong modulation on the scale of $c/(2\Delta)$, where c is a spin-wave velocity [8]. At the lower field (squares), there is larger modulation in the spin exciton (but $\Xi_{\mathbf{00}}(\mathbf{r})$ only decays to half its maximum value), and again the decay length of the charge correlations is about half that of the spin correlations. The spatial form of the lower field $\Omega(\mathbf{r})$ in Fig 3 is quite similar to envelope of the modulation observed in [1].

The STM experiments of [1] actually measure the modulation in the local electronic density of states (LDOS) in a range of energies as a function position in vortex lattice. A great deal of information is, in principle, contained in the energy and spatial dependence of the LDOS modulations. We have recently analyzed [8, 10] simple models for the coupling of the electronic quasiparticles to the collective SDW and SC degrees of freedom that have been discussed here: these lead to predictions for the LDOS modulations, which can be usefully compared with the STM data—the reader is referred to the papers for details.

We also mention here the recent STM experiments of Howald *et al.* [23] which have observed charge order similar to that of [1] but in zero applied magnetic field; this order has (presumably) been pinned by impurities.

2.2. STATIC SPIN MOMENT IN THE SC+SDW PHASE

The SC+SDW phase has $\langle \varphi_\mu \rangle \neq 0$, and hence via (1), (2), and (3), there is both static spin and charge order. Neutron scattering measurements have so far only succeeded in observing the static spin order, and so we will restrict our discussion here to the spin moment.

In the presence of an applied magnetic field, the vortex lattice will spatially modulate the value of $\langle \phi_\mu(\mathbf{r}) \rangle$, and this should, in principle, lead to satellite elastic peaks [19, 5, 9] surrounding the main elastic Bragg peaks at $\pm\mathbf{K}_x$, $\pm\mathbf{K}_y$ observed in neutron scattering. However,

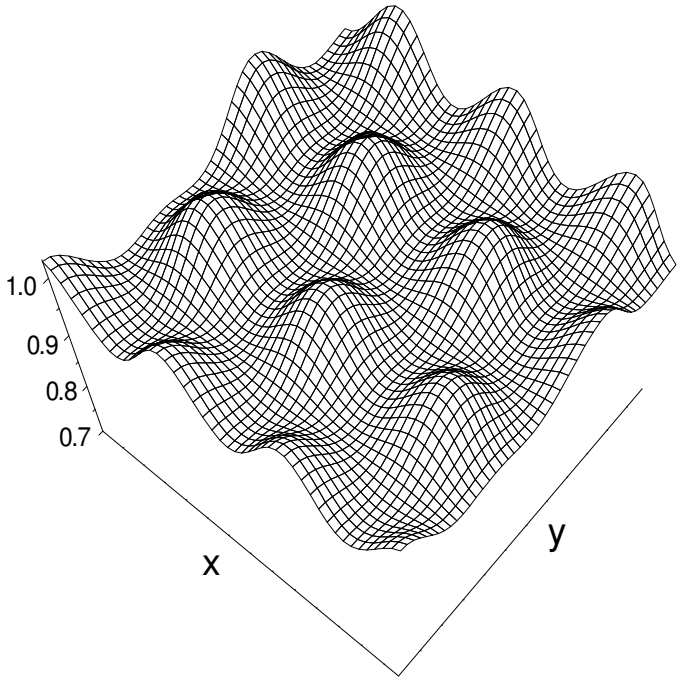

Figure 4. Spatial form of $\langle\varphi_\mu(\mathbf{r})$ in the SC+SDW phase. Notice the vertical scale, which shows that the overall modulation in the size of the order parameter is quite small. The numerical results were obtained by Ying Zhang and reported in [9].

our discussion above on the dominance of the superflow effect shows that this modulation occurs predominantly on the scale of the vortex lattice spacing [5, 9], and not on the scale of the vortex core. The resulting satellite peaks are consequently found to be extremely weak, as will be clear from our results below.

We show a sketch of the spatial form of $\langle\varphi_\mu(\mathbf{r})$ at a point in the SC+SDW phase in Fig 4. All the coupling constants in the theory are the same as those used for the results in Fig 3 for the SC phase. Only the parameters s and H are tuned to move the system between the SC and SC+SDW phases. The spatial Fourier transform of Fig 4 determines the strength of the elastic Bragg peaks that will be observed in neutron scattering. In particular, the dynamic structure factor of φ_μ has the form

$$S_\varphi(\mathbf{k},\omega) = (2\pi)\delta(\omega)\sum_{\mathbf{G}} |f_{\mathbf{G}}|^2 (2\pi)^2 \delta(\mathbf{k}-\mathbf{G}) \tag{15}$$

where $\mathbf{G}$ are the reciprocal lattice vectors of the vortex lattice. The reader should keep in mind, via (1) and (3), that the experimental structure factor is obtained from (15) by measuring wavevectors from

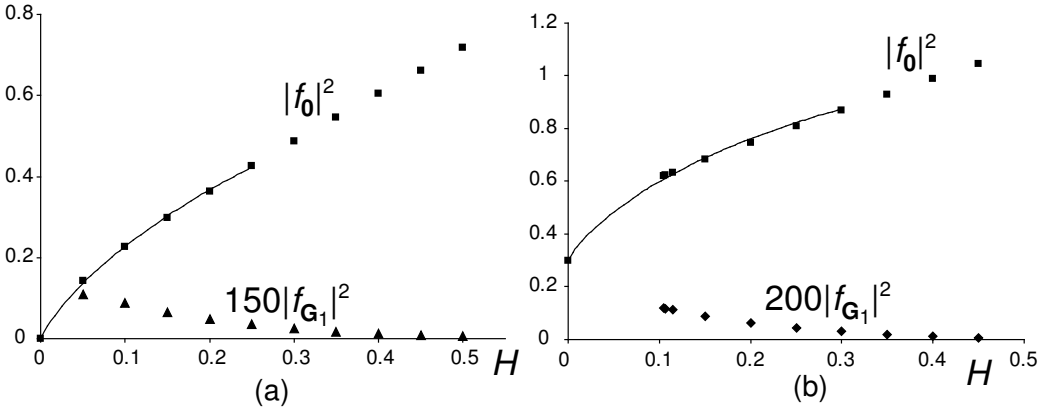

Figure 5. Magnitudes of the elastic scattering peaks in (15) obtained by the spatial Fourier transform of results like those in Fig 4. The field H is measured in units of H_{c2}^0, the value of the critical field at which all four phases meet in Fig 2. The plot (a) is at $s = s_c$, while (b) is for $s < s_c$. All other couplings are identical to those in Figs 3 and 4. The numerical results were obtained by Ying Zhang and reported in [9].

the SDW ordering wavevectors $\pm\mathbf{K}_x$, $\pm\mathbf{K}_y$. We show typical results for the field dependence of the strength of the central peak, $|f_{\mathbf{0}}|^2$, and also for the first satellite peak, $|f_{\mathbf{G}_1}|^2$ (where $\mathbf{G}_1$ is the smallest non-zero reciprocal lattice vector) in Fig 5. The strong observable effect is in the H dependence of the central peak $|f_{\mathbf{0}}|^2$. The same superflow effects which were responsible for (11), also dominate in determining the average magnitude of the SDW order in the SC+SDW phase: we can estimate the enhancement of magnetic order by the superflow by assuming that $f_{\mathbf{0}}$ is determined by s_{eff}, and then (10) leads to

$$|f_{\mathbf{0}}|^2(H) - |f_{\mathbf{0}}|^2(0) \propto H \ln(1/H). \tag{16}$$

the lines in Fig 5 are fits of the full numerical solution to (16). Arovas *et al.* [19] had discussed nucleation of static magnetic order in the vortex core in what was an SC phase. In contrast, we claim that there are *no static spins in the vortices in the SC phase*, and only pinned static charge order around each vortex as discussed in Section 2.1. The static moments appear only when there is bulk magnetic order as in the SC+SDW phase (as pointed out in [5, 9]), and here it is the contribution of the superflow which always dominates leading to (16). The linear small H dependence of the ordered moment proposed by Arovas *et al.* is not valid in either the SC or the SC+SDW phases.

The results in Fig 5 also compare well with the experimental observations in the overall scale of both the field and the magnetic moment: those in (a) are quite similar to the results of [2], while (b) matches well with [3].

Finally, note that Fig 5 shows that the satellite peaks are unobservably small. This is related to relatively slow modulation induced by the superflow in the moment in Fig 4. Ref. [9] predicted that the influence of the vortex lattice may be more easily observable in the *dynamic* exciton band structure in the SC phase.

3. WHY DOES THE CHARGE ORDER HAVE PERIOD 4 ?

The SDW ($\mathbf{K}_{x,y}$) and charge ($2\mathbf{K}_{x,y}$) ordering wavevectors have so far been arbitrary parameters in our phenomenological theory, and the structure of this theory is largely independent of the values of $\mathbf{K}_{x,y}$ (some high order terms in the action are permitted only for certain commensurate values of $\mathbf{K}_{x,y}$). The determination of $\mathbf{K}_{x,y}$ requires, instead, a lattice scale theory of the doped antiferromagnet.

The mechanism of the charge-ordering instability in doped antiferromagnets has been discussed using a number of different theoretical perspectives by several other workers [24, 25, 26, 27, 28]; in general, many possible charge-ordering periods emerge in their works, and there appear to be no fundamental principles restricting the possible periods, or whether the charge-ordering is site or bond centered. Here, we will briefly recall our theoretical work on charge ordering [4]: its point of departure is the theory of the magnetic quantum critical point in the Mott insulator. Our perspective led to bond-centered charge ordered states, without long-range magnetic order, and with co-existing d-wave-like superconductivity. The predicted evolution of the wavevector of this ordering, as a function of hole concentration, is shown in Fig 6. Note that the period, p, is always pinned to be an even number *i.e.* $2\mathbf{K}_x = (2\pi/a)(1/p, 0)$, where a is the square lattice spacing. There is a large range of δ values in Fig 6 where the period is pinned at $p = 4$: this corresponds to the values of $2\mathbf{K}_{x,y}$ observed in the STM experiments [1, 23]. Both experiments also see the modulation appearing simultaneously at $2\mathbf{K}_x$ and at $2\mathbf{K}_y$, leading to a checkerboard appearance in real space. Such checkerboard patterns have been considered previously for the $p = 2$ case [29, 30, 31, 32], and were found to have an energy very close to that of the state with charge order only along a single direction; we can expect that a similar result applies for $p = 4$.

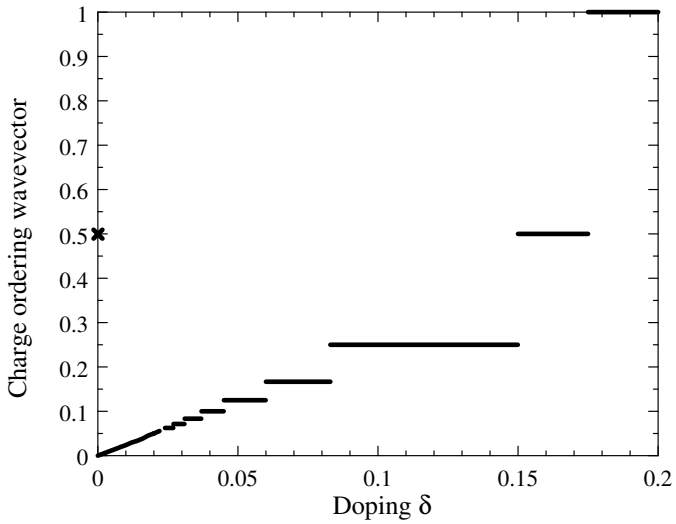

Figure 6. Evolution of the charge ordering wavevector upon doping a paramagnetic Mott insulator, from Ref. [4]. The wavevector is measured in units of $2\pi/a$. At $\delta = 0$, the Mott insulator has period 2, which is associated with the appearance of bond order (see Fig 7). Beyond a range of very small δ values, the ground state is also a superconductor. Full square lattice symmetry is restored above $\delta \approx 0.175$, when the ground state becomes an ordinary d-wave superconductor.

Further support for Fig 6 has emerged from recent neutron scattering measurements of Mook *et al.* [33] in the under-doped superconductor $YBa_2Cu_3O_{6.35}$: they observed static charge order, and dynamic spin correlations, with the the charge order period pinned rather precisely at $p = 8$. This is in accord with the plateau at $p = 8$ over a range of small δ values in Fig 6, and should be contrasted with the continuous evolution of ordering wavevector with δ which is usually assumed in the "Yamada plot" [34, 35] for periods larger than $p = 4$.

We conclude this paper by briefly recalling the physical ingredients behind the results in Fig 6. A review of these arguments has already been presented in [7], and we present here a synopsis in Fig 7. In moving from an undoped Mott insulator, like La_2CuO_4, to a high temperature superconductor at optimal doping, at least two quantum phase transitions must take place: one involving the loss of magnetic order, and the other the onset of superconductivity. Theoretically, it is very useful to disentangle the two transitions by imagining that we have a second tuning parameter at our disposal, in addition to the doping δ. We use this second parameter to first destroy the magnetic order in La_2CuO_4 while remaining at $\delta = 0$—a specific possibility for such a parameter

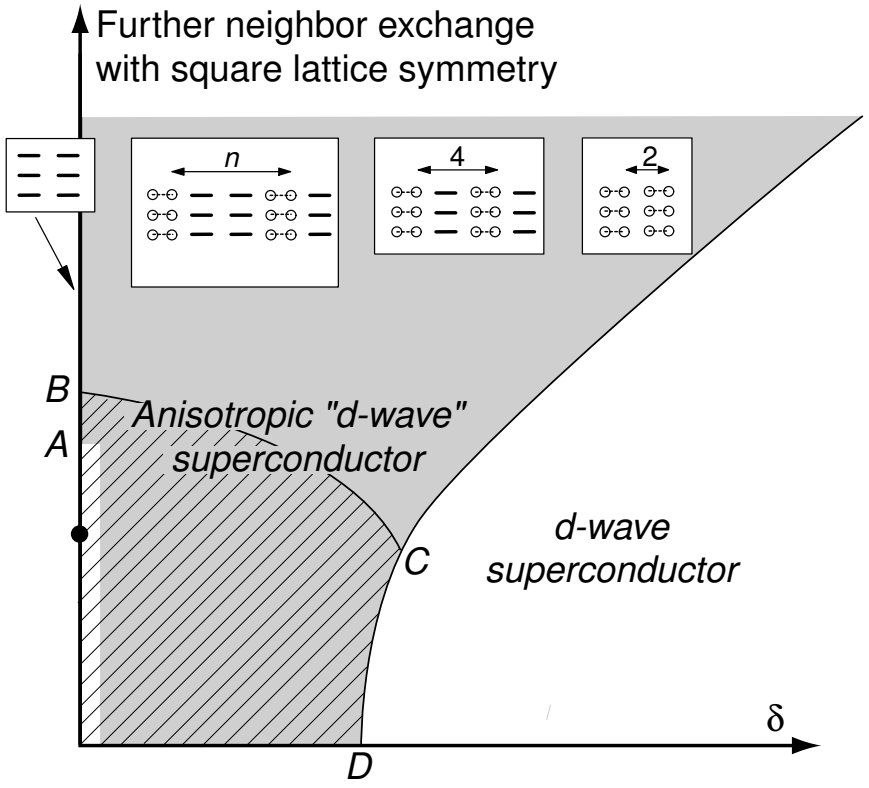

Figure 7. Schematic $T = 0$ phase diagram (from Refs. [4, 7]) for the high temperature superconductors as a function of a ratio of the near neighbor exchange interactions and the hole concentration, δ; *e.g.* the vertical axis could be J_2/J_1, the ratio of the first to second neighbor exchange. The shaded region has charge order. The hatched region has broken spin-rotation symmetry with $\langle \vec{S} \rangle \neq 0$, and at least one of the order parameters $\Phi_{x,y\alpha}$ is non-zero; $\langle \vec{S} \rangle = 0$ elsewhere. The unfrustrated, insulating antiferromagnet with long-range Néel order is indicated by the filled circle. At $\delta = 0$, there is an onset of charge order above the point A, while spin-rotation invariance is restored above B. The nature of the charge orders as determined by the computations of Ref. [4] are indicated at the top of the figure; numerous transitions, within the gray shaded region, in the nature of the charge ordering are not shown. The ground state at very low non-zero doping is an insulating Wigner crystal and there is subsequently a insulator-to-superconductor transition; superconductivity is present over the bulk of the $\delta > 0$ region. The central idea behind our approach is that many essential aspects the spin excitation spectrum of the insulating, paramagnetic region ($\delta = 0$, $\langle \vec{S} \rangle = 0$) lead to a simple and natural description of the analogous properties of the d-wave superconductor.

is a frustrating second neighbor exchange interaction (see Fig 7). Detailed arguments have been given (for a recent review see [36]) that the paramagnetic Mott insulator so obtained has bond-centered charge order, as indicated in Figs 6 and 7. The second theoretical step of doping the paramagnetic Mott insulator can be reliably addressed in a large N theory [4], and one eventually obtains a d-wave superconductor which fully respects the symmetries of spin rotations and lattice translations and rotations. In this approach, the charge order of the superconductor without magnetic long range order evolves from that in the paramagnetic Mott insulator. Further, the Cooper pairing in the superconductor is also connected to the singlet electron pairing present in the bond-ordered paramagnetic Mott insulator. These connections led us to the results in Fig 6, and to the proposal of charge order nucleation by vortices in [6].

Acknowledgments

The results reviewed here were obtained with Eugene Demler, Kwon Park, Anatoli Polkovnikov, Matthias Vojta, and Ying Zhang; I thank them for fruitful collaborations. This research was supported by US NSF Grant DMR 0098226.

References

[1] J. E. Hoffman, E. W. Hudson, K. M. Lang, V. Madhavan, S. H. Pan, H. Eisaki, S. Uchida, and J. C. Davis, Science **295**, 466 (2002).

[2] B. Lake, H. M. Rønnow, N. B. Christensen, G. Aeppli, K. Lefmann, D. F. McMorrow, P. Vorderwisch, P. Smeibidl, N. Mangkorntong, T. Sasagawa, M. Nohara, H. Takagi, T. E. Mason, Nature **415**, 299 (2002).

[3] B. Khaykovich, Y. S. Lee, S. Wakimoto, K. J. Thomas, R. Erwin, S.-H. Lee, M. A. Kastner, and R. J. Birgeneau, Phys. Rev. B **66**, 014528 (2002).

[4] M. Vojta and S. Sachdev, Phys. Rev. Lett. **83**, 3916 (1999); M. Vojta, Y. Zhang and S. Sachdev, Phys. Rev. B **62**, 6721 (2000); S. Sachdev and N. Read, Int. J. Mod. Phys. B **5**, 219 (1991).

[5] E. Demler, S. Sachdev, and Y. Zhang, Phys. Rev. Lett. **87**, 067202 (2001).

[6] K. Park and S. Sachdev, Phys. Rev. B **64**, 184510 (2001).

[7] S. Sachdev, Proceedings of Spectroscopies in Novel Superconductors, J. Phys. Chem. Solids **63**, 2269 (2002), cond-mat/0108238.

[8] A. Polkovnikov, S. Sachdev, M. Vojta, and E. Demler, Proceedings of PPHMF IV, World Scientific, Singapore, Int. J. Mod. Phys. B **16**, 3156 (2002), cond-mat/0110329.

[9] Y. Zhang, E. Demler, and S. Sachdev, Phys. Rev. B **66**, 094501 (2002).

[10] A. Polkovnikov, M. Vojta, and S. Sachdev, Phys. Rev. B **65**, 220509 (2002).

[11] S. Sachdev and J. Ye, Phys. Rev. Lett. **69**, 2411 (1992); A. V. Chubukov and S. Sachdev, Phys. Rev. Lett. **71**, 169 (1993).

[12] T. Imai, C. P. Slichter, K. Yoshimura, and K. Kosuge, Phys. Rev. Lett. **70**, 1002 (1993).

[13] G. Aeppli, T. E. Mason, S. M. Hayden, H. A. Mook, and J. Kulda, Science **278**, 1432 (1997).

[14] L. Balents, M. P. A. Fisher, and C. Nayak, Int. J. Mod. Phys. B **12**, 1033 (1998).

[15] A. V. Chubukov and S. Sachdev and J. Ye, Phys. Rev. B **49**, 11919 (1994); S. Sachdev and M. Vojta, Physica B **280**, 333 (2000).

[16] S. Sachdev, C. Buragohain, and M. Vojta, Science **286**, 2479(1999); M. Vojta, C. Buragohain and S. Sachdev, Phys. Rev. B **61**, 15152 (2000).

[17] O. Zachar, S. A. Kivelson, and V. J. Emery, Phys. Rev. B **57**, 1422 (1998).

[18] S.-C. Zhang, Science **275**, 1089 (1997).

[19] D. P. Arovas, A. J. Berlinsky, C. Kallin, and S.-C. Zhang, Phys. Rev. Lett. **79**, 2871 (1997); J.-P. Hu and S.-C. Zhang, J. Phys. Chem. Solids **63**, 2277 (2002).

[20] B. Lake, G. Aeppli, K. N. Clausen, D. F. McMorrow, K. Lefmann, N. E. Hussey, N. Mangkorntong, M. Nohara, H. Takagi, T. E. Mason, and A. Schröder, Science **291**, 1759 (2001).

[21] S. Sachdev, Phys. Rev. B **45**, 389 (1992); N. Nagaosa and P. A. Lee, Phys. Rev. B **45**, 966 (1992).

[22] Y. Chen and C. S. Ting, Phys. Rev. B **65**, 180513 (2002); J.-X. Zhu, I. Martin, and A. R. Bishop, Phys. Rev. Lett. **89**, 067003 (2002).

[23] C. Howald, H. Eisaki, N. Kaneko, and A. Kapitulnik, Proc. Nat. Acad. Sci. **100**, 17 (2003).

[24] S. R. White and D. J. Scalapino, Phys. Rev. Lett. **80**, 1272 (1998); Phys. Rev. B **61**, 6320 (2000).

[25] M. Bosch, W. v. Saarloos, and J. Zaanen, Phys. Rev. B **63**, 092501 (2001); J. Zaanen and A. M. Oles, Ann. Phys. (Leipzig) **5**, 224 (1996).

[26] S. A. Kivelson, E. Fradkin, and V. J. Emery, Nature **393**, 550 (1998); U. Low, V. J. Emery, K. Fabricius, and S. A. Kivelson, Phys. Rev. Lett. **72**, 1918 (1994).

[27] H. Tsunetsugu, M. Troyer, and T. M. Rice, Phys. Rev. B **51**, 16456 (1995).

[28] C. Nayak and F. Wilczek, Phys. Rev. Lett. **78**, 2465 (1997).

[29] N. Read and S. Sachdev, Nucl. Phys. B **316**, 609 (1989).

[30] T. Dombre and G. Kotliar, Phys. Rev. B **39**, 855 (1989).

[31] S. Sachdev, *Quantum Phase Transitions*, chapter 13, Cambridge University Press, Cambridge (1999).

[32] E. Altman and A. Auerbach, Phys. Rev. B **65**, 104508 (2002).

[33] H. A. Mook, P. Dai, and F. Dogan, Phys. Rev. Lett. **88**, 097004 (2002).

[34] J. M. Tranquada, J. D. Axe, N. Ichikawa, A. R. Moodenbaugh, Y. Nakamura, and S. Uchida, Phys. Rev. Lett. **78**, 338 (1997).

[35] K. Yamada, C. H. Lee, K. Kurahashi, J. Wada, S. Wakimoto, S. Ueki, H. Kimura, Y. Endoh, S. Hosoya, G. Shirane, R. J. Birgeneau, M. Greven, M. A. Kastner, and Y. J. Kim , Phys. Rev. B **57**, 6165 (1998).

[36] S. Sachdev and K. Park, Annals of Physics **298**, 58 (2002).